Available online at www.sciencedirect.com
SCIENCE DIRECT
Polymer 46 (2005) 3522–3527
polymer
www.elsevier.com/locate/polymer

# Phase morphology and impact toughness of impact polypropylene copolymer

Hongsheng Tan[a,b], Li Li[b], Zhineng Chen[b], Yihu Song[a], Qiang Zheng[a,c,*]

[a]*Department of Polymer Science and Engineering, Zhejiang University, Zheda Road 38#, Hangzhou, Zhejiang 310027, China*
[b]*SINOPEC Qilu Corporation Ltd, Plastics Institute, Zibo, Shandong 255400, China*
[c]*State Key Laboratories of Chemical Engineering, Polymer Reaction Engineering Division, Zhejiang University, Hangzhou, 310027, China*

Received 13 October 2004; received in revised form 23 January 2005; accepted 7 February 2005
Available online 21 March 2005

**Abstract**

Factors influencing the impact toughness of two impact polypropylene copolymers (IPC) with almost the same ethylene content, molecular weight and molecular weight distribution were studied by temperature gradient extraction fractionation (TGEF), scanning electron microscopy (SEM), nuclear magnetic resonance (NMR) and differential scanning calorimetry (DSC). The results indicate that poor interfacial adhesion between the disperse phase and the continuous matrix, larger dimensions and non-uniform distribution of disperse phases are main reasons for the low impact toughness of IPC B that possesses of a low content of ethylene–propylene segmented copolymer with long crystallizable PE and PP sequences as a compatibilizer between the disperse phase and the matrix.


*Keywords:* Impact polypropylene copolymer; Phase morphology; Impact toughness

## 1. Introduction

Polypropylene as an important thermoplastic is limited in many applications, especially at low temperatures, due to its low impact resistance. Its toughness might be improved by a variety of elastomers [1–5], by adding of nucleating agent to reduce the average dimensions of spherulites [6], and by copolymerization of propylene with ethylene or other olefins [7], among which the copolymerization with ethylene is one of the most useful and effective methods.

In a continuous process, isotactic polypropylene is produced in the first stage, and a rubbery ethylene–propylene copolymer phase is dispersed in the homopolymer matrix in the second stage [8,9]. The copolymer phase is used to improve the impact strength of the product at low temperatures [8]. Previous investigations of the composition, the chain structure and the micromorphology showed that the impact polypropylene copolymer (IPC) was a multiphase copolymeric system [10–16], consisting of an ethylene–propylene random copolymer, a series ethylene–propylene segmented copolymers with different sequence lengths of polyethylene (PE) and polypropylene (PP) segments and a propylene homopolymer [17–19]. The synthesis process decides the multidispersity of the copolymer composition [8].

Blends of immiscible polymers by melt mixing show ultimate properties generally poorer than their individual constituents because of the strong phase separation leading to a coarse phase structure and low interfacial adhesion. Incorporating a compatibilizer into a multiphase system generally leads to a fine phase structure and enhanced interfacial adhesion [20]. In IPC, some researchers proposed that the ethylene–propylene segmented copolymers with long sequences might behave as compatibilizer that enhances the interfacial adhesion between the disperse phase and the matrix [17,21]. However, direct evidence for the presence of the compatibilizer in IPC is still obscure.

In this study, we use temperature gradient extraction fractionation (TGEF), scanning electron microscope (SEM), nuclear magnetic resonance (NMR) and differential scanning calorimetry (DSC) to study the factors determining the toughness of the IPC and provide a direct evidence that the lack of ethylene–propylene segmented copolymer with long crystallizable sequences leads to the coarsening of disperse

* Corresponding author. Tel./fax: +86 571 87952522.
*E-mail address:* zhengqiang@zju.edu.cn (Q. Zheng).

0032-3861/$ - see front matter © 2005 Elsevier Ltd. All rights reserved.
doi:10.1016/j.polymer.2005.02.088

phase in the IPC and bad toughness of the material. We select two IPC samples with almost the same ethylene content, molecular weight and molecular weight distribution in order to explore the key factors that determine the impact toughness of IPC.

## 2. Experimental

### 2.1. Materials

A commercial grade of IPC A was produced by 'Spheripol' process of Basell Co.; another IPC B was a testing product in the same industrial equipment using a different spherical Zieglar–Natta catalyst. The first stage of the process produced propylene homopolymer in liquid propylene using two loops. For the ethylene–propylene copolymer (EPR) stage, i.e. second stage, it utilized gas fluidized bed reactor. The liquid propylene/polymer suspension from the first reactor was flashed to gas/solid conditions prior to entering the second stage [8]. It was copolymerized with ethylene so that the final product (IPC) was gained. The sample A used in this paper was a kind of basic resin for auto bumper compound and other compounds of auto toughened parts with good low-temperature toughness.

### 2.2. Fractionation of the IPC

A modified Kumagawa extractor was used to carry out a temperature-gradient extraction fractionation of the IPC. *n*-Octane was employed as solvent and eight fractions were collected by extracting 5 g of the sample at 30, 50, 60, 70, 80, 90, 100, 110 and 120 °C, respectively. Purified fractions were obtained after concentrating the extract solutions, precipitating the polymer, washing and drying the fractions in vacuum [17].

### 2.3. Measurements

#### 2.3.1. Molecular weight and molecular weight distribution

Molecular weight and molecular weight distribution were examined by high-temperature gel permeation chromatography (GPC) (GPC V2000, Waters Co.) at 150 °C and using 1,2,4-trichloro-benzene as solvent.

#### 2.3.2. Scanning electron microscopy (SEM)

Fracture surfaces of impact test specimens at −20 °C were etched in xylene for 15 h at 15 °C, and were observed by means of an electron microscope (HITACHI H-7000, with scanning accessory) after coating gold-palladium. An operating voltage of 25 kV and a magnification of 5000 were used.

#### 2.3.3. Nuclear magnetic resonance (NMR)

$^{13}$C NMR spectra of the fractions were measured on a Bruker DMX400 spectrameter at 100 MHz. Solutions (10 wt%) were prepared in *o*-dichlorobenzene. The spectra were recorded at 125 °C. Broadband decoupling and a pulse delay of 5 s were used. Typically 6000 transients were collected.

#### 2.3.4. Differential scanning calorimetry (DSC)

Thermal analysis of the fractions was performed on a Perkin–Elmer Pyris 1 thermal analyzer under a high purity nitrogen atmosphere at a rate of 10 °C/min. The samples in all of fractions were dealt with by multiple isothermal annealing at 130, 120, 110, 100, 90, 80, 70, 60 and 50 °C, respectively, each for 12 h.

#### 2.3.5. Intrinsic viscosity ratio

The intrinsic viscosity $[\eta]$ of the IPC was measured with a modified Ubbelhode type viscometer at 135 °C using decalin as solvent. A small amount of antioxidant was added in the solution [22]. The intrinsic viscosity ratio $\lambda$ was defined as the ratio of intrinsic viscosity $[\eta]_1$ of a xylene soluble component (EPR) to intrinsic viscosity $[\eta]_2$ of a xylene dissoluble component (including mainly PP matrix) in an IPC, i.e.

$$\lambda = \frac{[\eta]_1}{[\eta]_2}$$

Both components in the IPC were gained though hot dissolution of polymer samples in boiling xylene, followed by cooling to a temperature of 25 °C. Solid materials (xylene dissoluble component) were then removed through filtration and the remaining polymer solution were dried under vacuum. Solid residues containing the soluble polymer material are the xylene soluble component [23].

#### 2.3.6. Impact toughness

Notched izod impact tests of specimens injected at 230 °C were carried out by means of a Ceast pendulum impact tester at −20 and 23 °C, respectively, according to ISO180.1993. Five specimens of each sample were tested and the average values were reported.

## 3. Result and discussion

### 3.1. Molecular weight and impact toughness

Both IPC samples A and B have similar ethylene content, molecular weight and molecular weight distribution, but their impact toughness is very different, as shown in Table 1. The impact strengths of sample A are significantly higher than sample B.

### 3.2. Phase morphology

Fig. 1 shows SEM micrographs of impact fracture surfaces of both IPC pellets at low temperature after etching. Prominent spherical granules are dispersed in a PP matrix in

Table 1
Ethylene content, molecular weight and impact toughness of both IPC

| | A | B |
|---|---|---|
| Ethylene content (%) | 13.57 | 13.05 |
| $M_n \times 10^{-4}$ | 5.57 | 5.59 |
| $M_w \times 10^{-4}$ | 29.9 | 29.9 |
| Molecular weight distribution | 5.37 | 5.34 |
| Notched izod impact strength (kJ/m$^2$) | | |
| 23 °C | 48.20 | 11.60 |
| −20 °C | 10.48 | 6.57 |
| Intrinsic viscosity ratio ($\lambda$) | 2.17 | 1.67 |

the micrographs. Dimensions of both disperse phases in their matrices are similar (about 0.5–1 μm), while their distributions are slightly different. The distribution of disperse phases in sample A is more uniform than that of sample B. After the pellets were injected into test specimens, the disperse phases either in global or ellipsoidal domains become larger obviously. There are some sunken cavities and prominent granules, and something like thin threads between the granules in some cavities and the matrix, which reveals interfacial adhesion between the disperse phases and the matrix (Fig. 2). Such morphology couldn't appeared in the common blends of homopolypropylene filled with toughener [8,24]. The dimensions of the disperse phases in sample A are about 1–5 μm and their distribution in the matrix is apparently uniform. The dimensions of the disperse phases in sample B about 2–10 μm while their distribution is obviously inhomogeneous. It is clear that the sizes of the disperse phases in sample B are obviously larger than those in sample A.

### 3.3. Fractionation and chain structure

Fig. 3 shows weight contents of the fractions extracted at different temperatures, and Fig. 4 shows the DSC analysis of the various fractions during heating process. The contents of the 30 °C fractions in Fig. 3 are almost equal to each other in both IPC samples. There are no any melting peaks in these

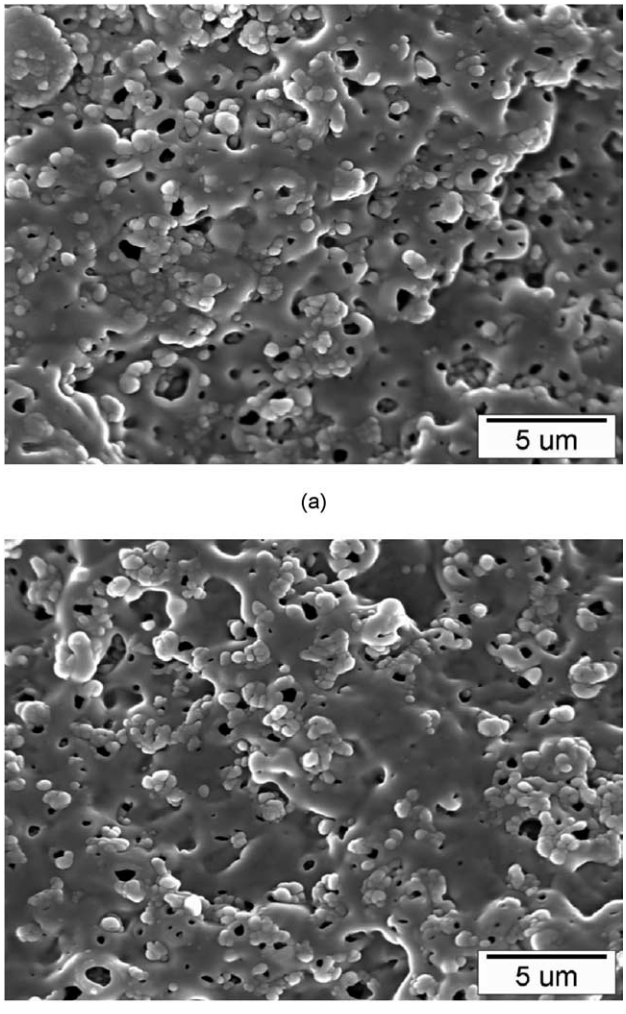


Fig. 1. SEM micrographs of fracture surface of the IPC pellets at −20 °C: (a) IPC A and (b) IPC B.

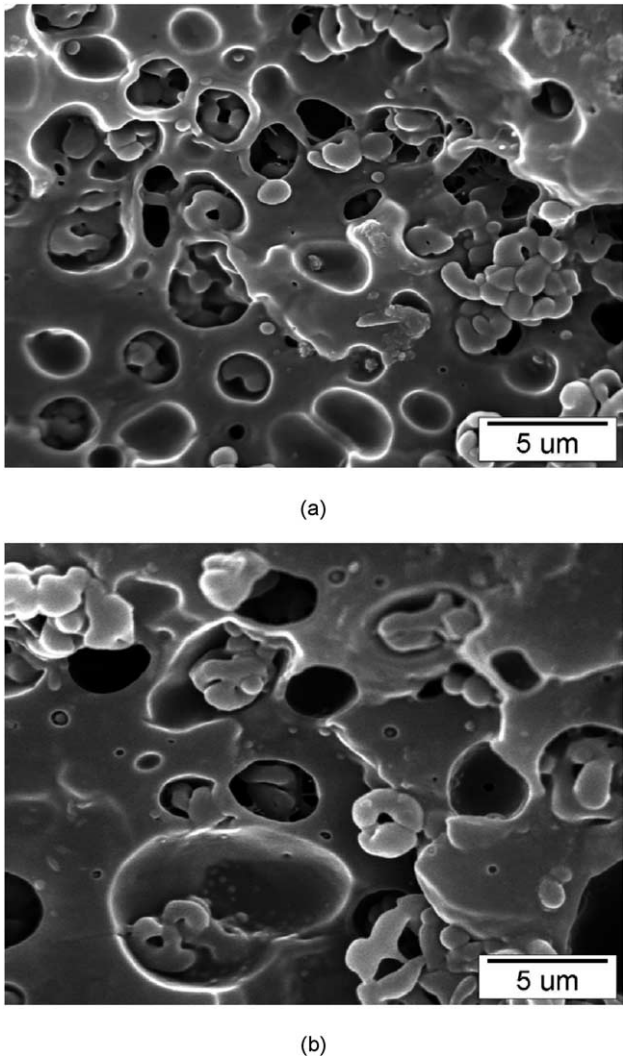


Fig. 2. SEM micrographs of fracture surface of the IPC impact specimens at −20 °C: (a) IPC A and (b) IPC B.

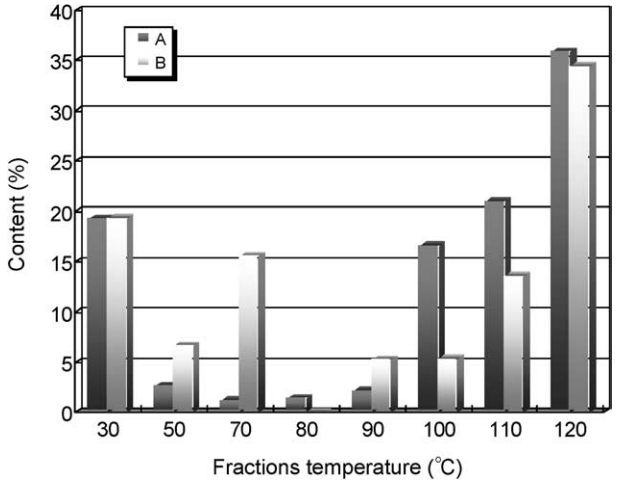


Fig. 3. Fractions distribution of both IPC.

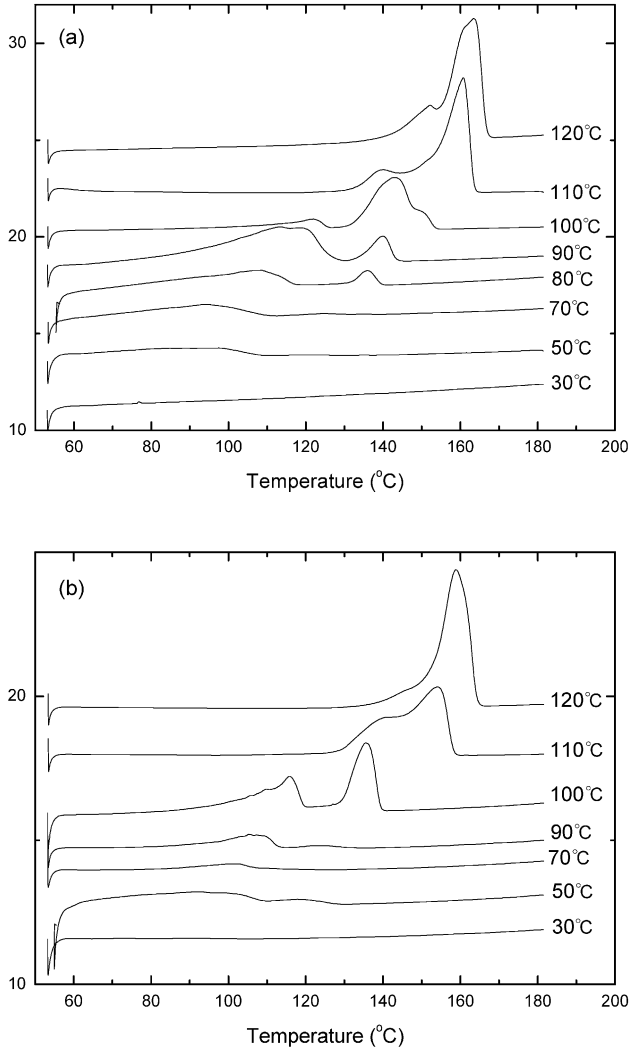


Fig. 4. DSC melting curves of all fractions in both IPC: (a) IPC A and (b) IPC B.

two 30 °C fractions in Fig. 4, revealing that they are mainly consisted of non-crystallizable ethylene and propylene segments as a kind of ethylene–propylene random copolymer.

In sample A, the 50 and 70 °C fractions do not show any melting peaks at temperatures above 130 °C, suggesting that there are almost no PP segments long enough to be crystallizable in these fractions. The 80 and 90 °C fractions with small contents of 1.4 and 2.1% show two melting peaks at 108 and 136 °C, and 117 and 140 °C, respectively, corresponding to the melting of crystalline PE and PP segments. The PP melting peaks in both fractions are relatively small because the crystallizable PP segments are not long enough. In the 100 °C fraction with a content of 16.6%, PP segment is long enough to form crystal with a melting peak centered at 143 °C. The 110 and 120 °C fractions possess a main melt peak at 161 and 164 °C, and a weak shoulder peak at 139 and 152 °C, respectively, which means that PP with long sequences is the main constitute in these two fractions.

In sample B, the 50 °C fraction does not show obvious melting characteristic in the whole temperature range of DSC test while the 70 °C fraction exhibits a tiny peak at ~100 °C possibly contributing to the melting of PE crystals with considerable imperfection. In the 90 °C fraction, a distinct PE melting peak located at 108 °C suggests the presence of crystallizable PE sequences. The 100 °C fraction also gives rise to a distinct melting peak at 116 °C, while a high-temperature peak at 140 °C due to PP melting coming into appearance. The fusion enthalpy of the high-temperature peak is obvious higher than that of the low-temperature peak. The 110 °C fraction shows a main peak at 154 °C and a shoulder at 140 °C, both assigned to PP crystals. The 120 °C fraction gives rise to a broad single peak with the peak temperature at 159 °C.

$^{13}$C NMR spectra of the 90, 100 and 110 °C fractions in sample A and the 110 °C fraction in sample B were measured to order to clarify their composition and chain structure. The results are summarized in Table 2. In the 90 °C fraction of sample A, the content of triad PPP is considerably smaller than that of triad EEE, explaining the melting peak at 140 °C with an area smaller than the melting peak at 117 °C assigned to PE crystals. The contents of ethylene (E) and triad EEE in the 90 °C fraction are obviously higher than those of propylene (P) and PPP, respectively which agrees with the fact that the PE melting peak is obviously larger in area than the PP peak. In the 100 °C fraction of sample A, the PPP content is larger than EEE so that this fraction exhibits a main melting peak at 144 °C and a small peak at 122 °C. The 90 and 100 °C fractions can thus be considered as segmented copolymers consisting of crystallizable PP and PE segments. The small amounts of PEP, EPE, PEE and PPE sequences actually reveal the existence of transition segments between long PP and PE segments. The 110 °C fraction in sample A contains 98.49% triad PPP and very low contents of the other chain

Table 2
Sequence distribution (wt%) and tacticity (wt%) in the fractions for both IPC

| | A-90 °C | A-100 °C | A-110 °C | B-110 °C |
|---|---|---|---|---|
| E | 76.70 | 24.84 | 1.36 | 5.88 |
| P | 23.30 | 75.16 | 98.64 | 94.12 |
| EE | 72.87 | 23.66 | 1.25 | 5.20 |
| PE | 9.59 | 2.96 | 0.26 | 1.72 |
| PP | 17.54 | 73.38 | 98.49 | 93.08 |
| PEP+EPE | 4.7 | 1.71 | 0.18 | 1.26 |
| PEE | 6.72 | 1.43 | 0.14 | 0.59 |
| EEE | 69.51 | 22.94 | 1.18 | 4.90 |
| PPE | 3.04 | 1.07 | 0.00 | 0.33 |
| PPP | 16.02 | 72.85 | 98.49 | 92.92 |
| Tacticity | 90.75 | 95.93 | 97.40 | 97.80 |

sequences, which is the reason that this fraction exhibits a marked melting peak at 161 °C. The melting temperature is slightly lower than pure PP crystals because of the existence of the short PE segments or ethylene mers in the macromolecular chains. A weak PP peak at 140 °C might correspond to crystals from somewhat short crystallizable PP segment interrupted by short PE segments or ethylene mers. The 110 °C fraction in sample B contains triad PPP and EEE of 92.92 and 4.90%, respectively. The ethylene sequences could not crystallize while it makes the PP segments considerably shorter in comparison with those in sample A. This is the reason that the melting point of the 110 °C fraction in sample B is lower than that in sample A.

Table 3 shows the fusion enthalpy of the PP melting peak in the 50, 70, 80 and 90 °C fractions for both samples A and B. The fusion enthalpy of the 50 °C fraction in sample A is zero, and that of the 70 °C fraction is very small (1 J/g). The fusion enthalpies of the 50, 70 and 80 °C fractions in sample B are zero and that of the 90 °C fraction is very low. From this analysis, it is concluded that the 30, 50 and 70 °C fractions with a sum content 24.51% might be mains of the disperse phase in sample A, while the 30, 50, 70 and 90 °C fractions with a sum content 41.51% form mainly the disperse phase in sample B. The content of the disperse phase in sample B is obviously higher than that in sample A.

### 3.4. Influence of compatibilizer content on the toughness

Generally, main factors influencing the IPC toughness might include the composition of the resin; molecular weight, molecular weight distribution and tacticity of matrix; the composition, structure, content and dispersion morphology of disperse phases and the compatibility between the matrix and disperse phase, etc. Long PP segments in ethylene–propylene segmented copolymer are highly compatible with isotactic PP, and the PE segments in the segmented copolymer are compatible with the PE segments in the disperse phase. The segmented copolymer acts as a compatilizer between the disperse phase and the matrix, resulting in strong interactions between the two phases [17], small dimension and uniform distribution of the disperse phase. The impact toughness is thus highly improved.

The dispersion of disperse phase in multiphase systems depends on the viscosity and compatibility between both phases [25]. The more similar are the viscosities of the xylene soluble and dissoluble components, the better is the dispersion of disperse phase in the IPC, i.e. the smaller is the dimension of the disperse phase. In Table 1, the intrinsic viscosity ratio ($\lambda_B = 1.67$) of sample B is obviously smaller than that ($\lambda_A = 2.17$) of sample A, which suggests that the dispersity of sample B should be better than sample A. However, the SEM photographs in Fig. 2 show the contrary result. Therefore, the dispersion of rubbery component in the matrix could not be explained on the basis of the intrinsic viscosity ratio. On the other hand, the compatibility between the components in IPC might be a key factor that determines the dispersion of disperse phase and the toughness.

In sample A, the 80, 90 and 100 °C fractions with a sum content of 17.81% have crystallizable PP and PE segments as judged from DSC analysis. These fractions as ethylene–propylene segmented copolymers contribute to improve adhesion between the matrix and the disperse phase. They could cover the disperse phase during in injection processing at elevated temperatures and prevent the isolated microdomains from aggregation, resulting in the apparently uniform morphology as shown in Fig. 2(a). In sample B, only the 100 °C fraction exhibits two obvious melting peaks from PE and PP crystals, respectively, (Fig. 4(b)). The

Table 3
Area ($\Delta H_f$) of PP melting peaks (J/g) for the fractions of both IPC in DSC curves

| | 50 °C | 70 °C | 80 °C | 90 °C |
|---|---|---|---|---|
| A | 0 | 1 | 6.7 | 12.3 |
| B | 0 | 0 | 0 | 1.3 |

content of this fraction (5.34%) as compatilizer is very much smaller than the content of compatilizers in sample A. This is the reason that the interfacial adhesion in sample B is weaker than in sample A, and the disperse phases might aggregate easily during processing, leading to a coarse and non-uniform distribution of the disperse phases as shown in Fig. 2(b). The content of disperse phases in sample B is obviously higher than sample A, which is advantageous for improving toughness of sample B. However, small compatibilizer results in the non-uniform distribution of disperse phases, which actually is the determining disadvantageous factor of the low impact toughness.

## 4. Conclusion

Two IPC with similar ethylene content, molecular weight and molecular weight distribution were studied in relation to the impact toughness, phase morphology, the melting behaviour and the NMR sequence distribution. It was found that bad interface adhesion between the disperse phase and continuous matrix, larger dimension and non-uniform distribution of disperse phases are main reasons that lead to weak toughness for sample B. The low content of ethylene–propylene segmented copolymer with long PE and PP sequences as radical reason leads to the poor compatibility between disperse phase and matrix, and bad toughness for sample B.

## Acknowledgements

The authors wish to thank Prof Zhiqiang Fan, at Zhejiang University, People's Republic of China, for TGEF, DSC and NMR measurements.

## References

[1] Greco R, Mancarella C, Martuscelli E, Ragosta G, Yin J. Polymer 1987;28:1929–36.
[2] D'Orazio L, Mancarella C, Martuscelli E, Sticotti G. J Mater Sci 1991;26:4033–47.
[3] Tam WY, Cheung T, Li RKY. Polym Test 1996;15:363–79.
[4] Zhang XF, Xie F, Pen ZL, Zhang Y, Zhang YX, Zhou W. Eur Polym J 2002;38:1–6.
[5] McNally T, McShane P, Nally GM, Murphy WR, Cook M, Miller A. Polymer 2002;43:3785–93.
[6] Premphet K, Horanont P. Polymer 2000;41:9283–90.
[7] Rosa CD, Auriemma F, Vinti V, Grassi A, Galimberti M. Polymer 1998;39:6219–26.
[8] Debling JA, Zacca JJ, Ray WH. Chem Eng Sci 1997;52:1969–2001.
[9] Prasetya A, Liu L, Litster J, Watanabe F, Mitsutani K, Ko GH. Chem Eng Sci 1999;54:3263–71.
[10] Cheng HN, Lee GH. Macromolecular 1987;20:436–40.
[11] Hayashi T, Inoue Y, Chllio R. Polymer 1988;29:1848–57.
[12] Francis M, Mirabella J, Douglas C. Polymer 1996;37:931–8.
[13] Cai HJ, Luo XL, Ma DZ, Wang JM, Tan HS. J Appl Polym Sci 1999; 71:93–101.
[14] Hansen EW, Redford K, Øysæd H. Polymer 1996;37:19–24.
[15] Nitta K, Kavada T, Yamahiro M, Mori H, Terano M. Polymer 2000; 41:6765–71.
[16] Sun Z, Yu F, Qi Y. Polymer 1991;32:1059–60.
[17] Fan ZQ, Zhang YQ, Xu JT, Wang HT, Feng LX. Polymer 2001;42: 5559–66.
[18] Fu ZS, Fan ZQ, Zhang YQ, Feng LX. Eur Polym J 2003;39:795–804.
[19] Xu JT, Feng LX, Yang SL, Wu YN. Polymer 1997;38:4381–5.
[20] Horák Z, Fořt V, Hlavatá D, Lednický F, Večerka F. Polymer 1996; 37:65–73.
[21] Cai HJ, Luo XL, Ma DZ, Wang JM, Tan HS. J Appl Polym Sci 1999; 71:103–13.
[22] Xu JT, Feng LX. Eur Polym J 1999;35:1289–94.
[23] Latado A, Embiruçu M, Neto AGM, Pinto JC. Polym Test 2001;20: 419–39.
[24] D'Orazio L, Mancarella C, Martusceli E, Cecchin G, Corrieri R. Polymer 1999;40:2745–57.
[25] Hong DY, editor. Polypropylene–mechanism, process and technology. Beijing: China Petrochemical; 2002. p. 506 [Chinese].